The EU Framework Programme for Research and Innovation H2020
Research and Innovation Action

Deliverable D2.3 First Prototype of Centauro Robot

Dissemination Level: Public

Project acronym:	CENTAURO
Project full title:	Robust Mobility and Dexterous Manipulation in Disaster Response by Fullbody Telepresence in a Centaur-like Robot
Grant agreement no.:	644839
Lead beneficiary:	IIT – Fondazione Istituto Italiano di Tecnologia
Authors:	Navvab Kashiri, Lorenzo Baccelliere, Luca Muratore Nikos Tsagarakis
Work package:	WP2 – Robot Platform
Date of preparation:	2017-10-23
Type:	Report
Version number:	1.0

Document History

Version	Date	Author	Description
0.1	2017-10-12	Navvab Kashiri, Lorenzo Baccelliere and Nikos Tsagarakis	Initial version
1.0	2017-10-23	Navvab Kashiri, Lorenzo Baccelliere and Nikos Tsagarakis	Submitted version

Executive Summary

Deliverable D2.3 presents the first prototype of the Centauro robot, a central element of the CENTAURO disaster-response system. The robot has an anthropomorphic upper body with two 7 DoF arms, a sensor head, and two five-finger hands. Its lower body consists of four articulated legs ending in steerable wheels. The deliverable details the robot design, its compliant actuation, assembly, and control software architecture.

Contents

1 Introduction

The workpackage WP2 focuses on the development and experimentation of the CENTAURO robot platform. To this end, the main target of the workpackage is to design and fabricate all mechanical and electrical components, and eventually assemble them to realize the first CENTAURO robot prototype in two design iterations.

In particular within WP2, the main goal of the Task T2.1 is the design and realization of the CENTAURO robot, while that of the Task T2.2 is the construction and assembly of the robot platform. Based on the project objectives and desired functionalities, including locomotion and manipulation in unstructured workspaces, payload capacity, and interaction with the environment, the robot specifications were derived and the design requirements were defined. To achieve this, the design activity started during the first period of the project, and following to the development of CENTAURO upper body, the robot lower-body was devised. This comprises of the development of compliant actuation system powering the the robot joints, including both arm and leg actuators, as well as the design and realization of a torso module, two manipulator arms, four wheeled legs, and a head encompassing the major part of the robot perception unit. As an outcome of the aforementioned tasks T2.1 and T2.2, the first prototype of the CENTAURO robot is released.

This report describes the design, construction and the interfaces of the robot prototype. The document presents description and details on the solution employed for the realization, construction, and implementation of the robot limbs, as well as the integration of the dual arm upper-body with the wheeled quadrupedal lower-body and the head.

2 Centauro Robot Kinematics

2.1 Head

The head subsystem is placed on top of the torso unit, and encompasses a set of cameras and sensors. It includes:

- A two-DOF mobility platform for a Kinect 2 sensor, at the bottom layer, to generate yaw and pitch motions of this RGB-D sensor, respectively;
- A structure for an array of three colour cameras (PointGrey BlackFly BFLY-U3-23S6C wide angle cameras), at the middle layer, to install these cameras to the head base; and
- A continuous rotation single DOF support beam for a 3D LiDAR sensor (Velodyne PUCK sensor), at the top layer, to provide spherical coverage of the environment around the robot.

2.2 Torso

The torso unit incorporates two seven-DOF arms; in addition to a single DOF accommodated in the pelvis structure for the waist motion, to endow the upper-body with yaw rotation.

The kinematics of each of the two arms of the bi-manual system closely resembles an anthropomorphic arrangement to enable the upper body the capability of manipulating the environment with high dexterity. It comprises of three DOFs at the shoulder, one DOF at the elbow and another three DOFs at the wrist, Fig. 1. It therefore possesses one degree of redundancy in each of the arms to overcome the constraints that may be introduced in the

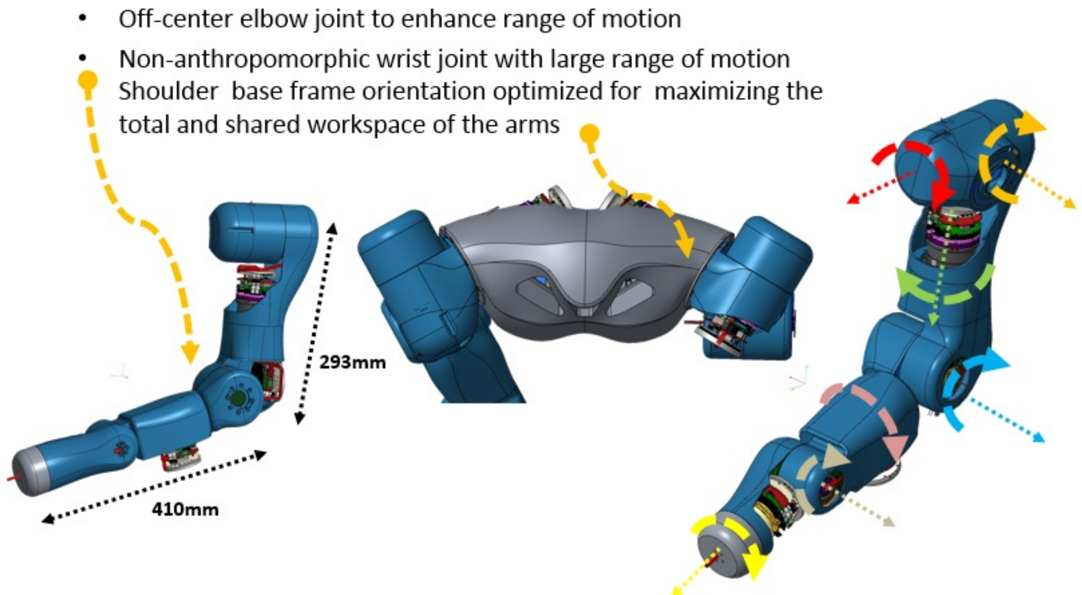

Figure 1: Arm kinematic features.

task space by the surrounding environment. Even though this is a traditional design that aims at replicating the anthropomorphic structure of the human arm with seven DOFs, it is only approximately equivalent for the human arm kinematic structure. To extend the range of motion of the elbow joint, an off-centre elbow configuration was considered. Similarly, for the wrist joint, a non-anthropomorphic configuration with non-intersecting axes was considered to maximise the range of motion of the wrist flexion and abduction motions. Finally humans have the ability to elevate (upward/downward) and to incline (forward/backward) the shoulder joint, utilising supplementary kinematic redundancy of the arm to achieve certain goals in task coordinates. This however would require the addition of two more DOFs for each arm, thereby increasing the complexity/weight and dimensions of the overall platform. To avoid this, while at the same time obtain, to some extent, the benefits provided by the elevation (upward/downward) and inclination (forward/backward) of the shoulder, a fixed elevated and inclined shoulder arrangement was selected based on the optimisation study in which important manipulation indices were considered and evaluated in a prioritized order.

The range of motion for the joints of the arm were defined considering human ergonomic data, data from other successful humanoid bi-manual systems and simulation studies of a number of manipulation tasks. The range of motion of the standard human arm was used as a starting point. Wherever it was possible, a greater range of motion with respect to human arm range was considered to enhance the motion and manipulation capability of the arm. In particular, the range of upper and lower arm rotations were extended. Similarly the range of elbow joint was increased by considering an off-centre elbow joint arrangement that results in a wide elbow flexion with respect to human elbow flexion. Finally the wrist flexion joint range was also extended to provide a larger range than that of the human wrist flexion, Fig.1.

2.3 Lower-body

The lower-body comprises of four wheeled legs whose first joints are accommodated in the four corners of the pelvis structure. To permit the versatile locomotion functionality, CENTAURO legs will consist of six DOFs based on the spider-like configuration. The spider leg configuration can be more beneficial in terms of stability required for manipulating powerful tools [3]. Furthermore, the first leg joint of the robot in this configuration will have to deliver substantially lower effort and power than that in mammal-like configuration. Based on the spidar joint principle the hip module of leg consists of two DOFs enabling the yaw and the pitch motions of the thigh body, respectively. Following the hip module, one additional DOF provides the pitch mobility for the knee. The ankle module of the leg consists of two DOFs that permit the pitch and yaw motion of the foot. Finally the last DOF of the leg is dedicated to the wheel that installed at the foot level allowing the robot to demonstrate also wheeled based mobility in addition to the articulated locomotion.

The design of the leg follows the same design principles described above for the arms. To permit versatile leg articulation in difficult terrains the range of the leg joints are maximized taking into account only the mechanical and electrical interfacing constraints.

3 Centauro Robot Actuation

3.1 Actuation Dimensioning

Having defined the kinematics of the arms, the next step was to identify the actuation performance required to satisfy the requirements defined in KHG meeting [4]. To estimate the actuation needs we execute a series of simulation studies using an initial model of the robot based on estimated rigid body dynamics properties. The Gazebo simulator is employed and the upper-body model and dynamics was implemented, see [1]. A set of harmonic trajectories with different frequencies are set as the reference joint trajectories in a way that the overall workspace of the arm is explored while carrying the 10 kg payload per arm. The evolution of joint torques is examined, based on which, five sizes of actuators respecting the individual torque requirements of the different arm joints were developed.

3.2 Actuation design

The realisation of the robot was based on the integration of seven series elastic actuator (SEA) units per arm, one SEA powering the torso, and six SEA units per legs; in addition to three conventional actuators in the robot head. The SEA technology is used to protect the reduction gear against impacts improving the system sturdiness while at the same time it is used for measuring the actuator torque through the monitoring of the elastic element deflection. The actuation units are realised based on two main assemblies: one consists of a Kollmorgen frameless brushless DC motor and the other includes a Harmonic Drive (HD) gearbox and the torque sensor unit. The actuators employ a 19-bit Renishaw magnetic encoder measuring the absolute rotor position and serving the Field Oriented control (FOC) implemented on the motor driver, and a 19-bit Renishaw magnetic encoder for measuring the absolute link position.

3.3 Joint torque sensing Principles

Considering the influence of different joints' stiffness level on the natural dynamics of the robot [6], and taking into account the available space in the different size actuators, two technologies were utilised for joint torque measurement based on strain-gauge and deflection-encoder principles for the small and medium size actuators as shown in Fig. 2, respectively, see [5]. The stiffness of SEA deflection-encoder-based sensor is defined with respect to the required torque measurement resolution across the different joints. It was set to 10 times lower than the

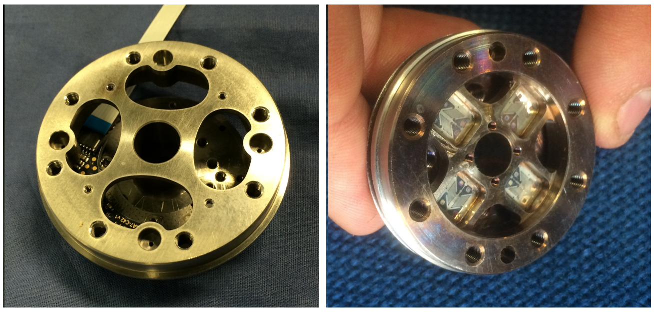

Figure 2: The deflection-encoder (left) and strain-gauge based torque sensors (right).

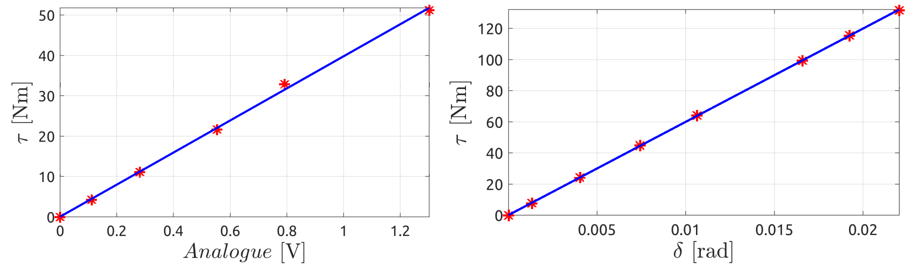

Figure 3: Calibration results of the two sensors: strain-gauge-based sensor on top, deflection-encoder-based sensor at the bottom. Red stars are collected experimental data, and blue lines are the corresponding filtered line.

cogging torque of the motor drive of the joint. The deflection of this sensor is measured using a high resolution absolute encoder of 19 bits.

Following the assembly of the actuator an identification process was carried out to verify the response of the sensors subject to external loading and derive their precise stiffness level and sensitivity. Fig. 3 shows a typical response of one of the two actuator sizes (medium) demonstrating linear behaviours and a stiffness level of 6009 Nm/rad for deflection-encoder based sensor and a voltage sensitivity of 39.7 Nm/V.

4 Centauro Robot Body and Assembly

4.1 Body Design Principle

The robot design followed an exoskeleton structure approach to connect the actuators to body structures. Exoskeleton cells have higher structural stiffness and minimize the effect of unmeasured elasticities. Fig. 4 illustrates the principle of the structure and actuation integration, in which the body of the actuators are floating inside this exoskeleton structure while the actuator is fixed to the link structures. As it can be seen, the actuation modules are mechanically interfaced to the exoskeleton cell links using two standard flange interfaces, one fixed to the previous link and the other to the subsequent link.

The exoskeleton structure and floating actuation integration approach offers several advantages with respect to the more traditional exoskeleton interconnection between the actuators and the robot links. Actuator bodies are not subject to loading as torques and forces generated from the joint loading or due to interactions, are transmitted only through the two output flanges used to fix the actuator to the structure cell. It therefore allows for optimal and low-weight design of the actuation housing components that are not subject to the joint loading.

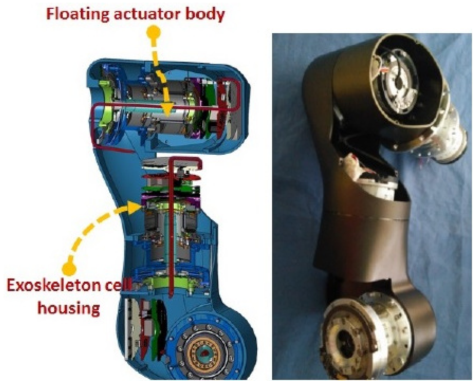

Figure 4: The exoskeleton cell structures and floating body principle.

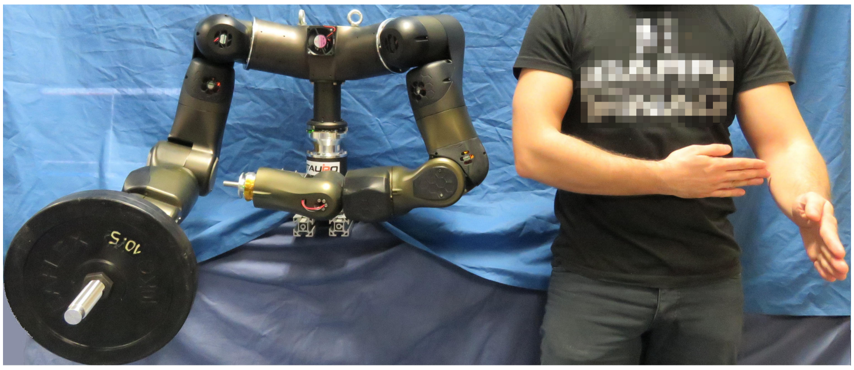

Figure 5: CENTAURO arm size comparison against an average human arm.

It is an explicit design feature that the link cells form a wind tunnel around the actuation body that can be used for forced air cooling.

4.2 Prototype Fabrication and Assembly

Based on the design principles described above, the mechanical components of the robot prototype were fabricated. The cell parts of the link structures were made from Aluminium T6-7075. The same material was used for the housing components of the harmonic gearbox and the interface flanges used to connect the actuation modules to the link structures. The mechanical components belonging to the floating part of the actuation body that are not subject to loading were machined using Magnesium Alloy AZ91 to minimize the weight of the actuation modules. The series elastic modules of the actuation system were made using Titanium Alloy that combines high strength with increased elasticity. Finally a number of no structural maintenance cover parts were made from ABS plastic using rapid prototyping fabrication. The first release of the full robot prototype that was pursued in two steps. First, the robot upper-body including the waist and two arms was released and experimented. It is shown in Fig. 5 as compared to an adult subject of a height of 1.78m.

Following to successful evaluation of the torso unit, the head and lower-body design including four wheeled legs was finalised and the body was fabricated and finally assembled. Fig. 6 shows the head assembly together with corresponding sensors and cameras. To endow the LiDAR laser scanner beam with continuous rotation, a slip ring device has been employed for the transmission of the LiDAR data and power. Fig. 7 demonstrates the first CENTAURO robot prototype. To full prototype is realised when the CENTAURO head is mounted on the torso

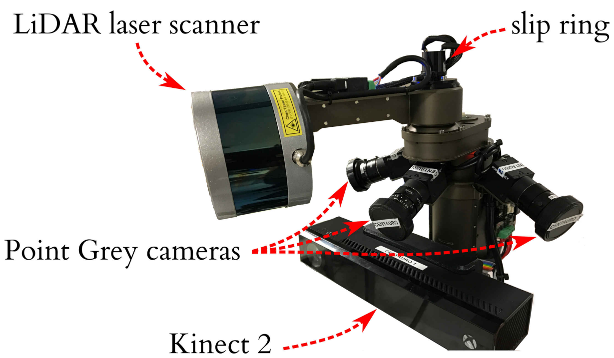

Figure 6: An image of the CENTAURO robot head module.

unit shown in Fig. 5, and the upper-body is installed on the wheeled quadrupedal platform. Furthermore, two commercial robotic hands (Schunk hand and SoftHand modules) are through the distal flange of the arms that provides an easy to adapt mechanical interface that can be tuned to match the mounting interface of these commercial systems; when communication and power cabling has been already taken into account in the arm design.

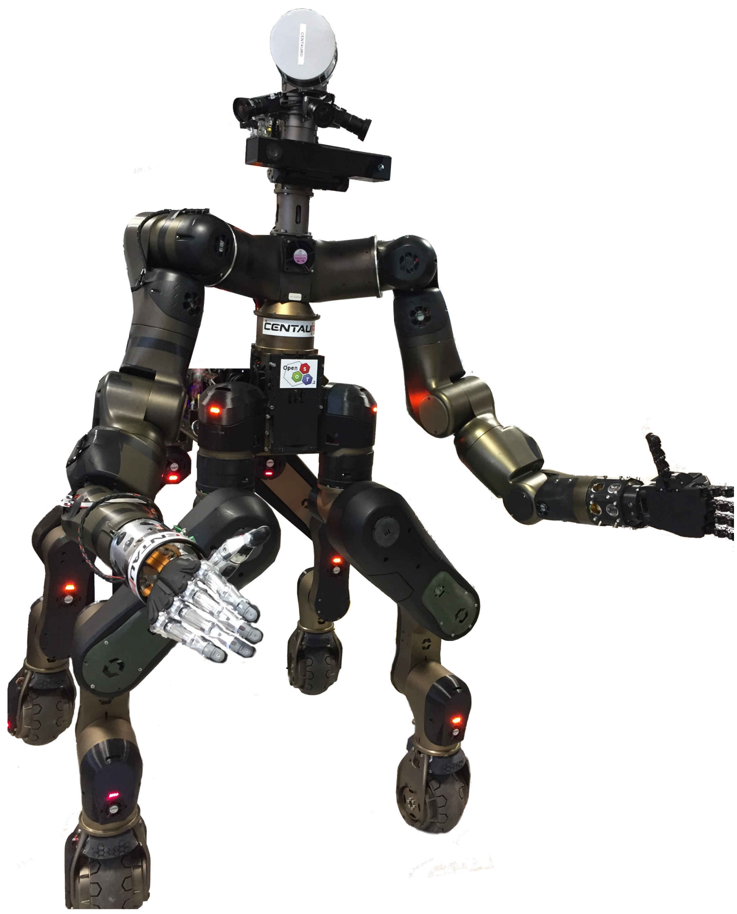

Figure 7: The first robot prototype.

5 Centauro Robot Control Architecture

While the lower-level joint controllers are executed on a dual-core microcontroller of individual actuators, the middle layer and higher-level control architecture of the CENTAURO robot relies upon four computation units: a COM Express module as motion PC, two Steam Box machines handling Vision/Perception data and higher-level controllers, and a Desktop computer as pilot PC. A high level schematic of the interconnections of the prototype control, actuation and perception components is shown in Fig. 8. The communication of the higher-level controllers

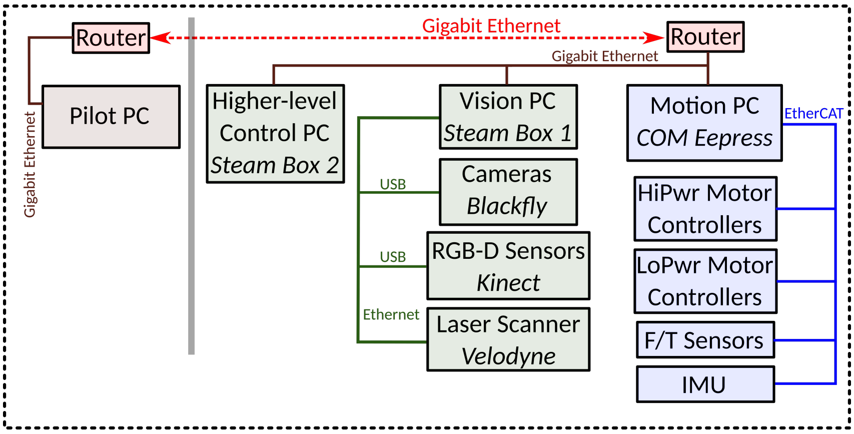

Figure 8: High level schematic of the interconnections of the CENTAURO prototype control, actuation and perception components.

with onboard PCs including Motion PC and Perception/Vision PCs is through a GigaBit Ethernet interface. The motion PC manages the data-broadcasting and centralized actuator control via real-time EtherCAT communication with both high and low power actuators' controllers, the Inertial Measurement Unit (IMU) and the Force/Torque (F/T) sensors. The vision PC is dedicated to the vision sensors acquisition, including three Point Grey Blackfly cameras, a kinect-2 R-GBD sensor and a Velodyne LiDAR laser scanner, through USB and Ethernet connections.

5.1 Real Time software Architecture

For the control of high performance bi-manual platform we have recently developed XBotCore (*Cross-Bot-Core*), a light-weight, Real-Time (RT) software platform for EtherCAT based robots [8]. XBotCore is open-source and is designed to be both an RT robot control framework and a software middleware. It satisfies hard RT requirements, ensuring 1 KHz hard real time control loop even in complex multi-DOF systems. Moreover it provides a simple and easy-to-use middleware Application Programming Interface (API), for both RT and non-RT control frameworks: XBotCore API is completely flexible with respect to the external control framework the user wants to utilise. As shown in Fig. 9, XBotCore components are the following: EtherCAT master, Plugin Handler, RT and non RT middleware API, Communication Handlers.

5.2 Actuation Control

The decentralised controller of the actuators is developed based on an impedance control scheme utilising motor positions θ and velocity $\dot{\theta}$, and measured joint torque τ, displayed

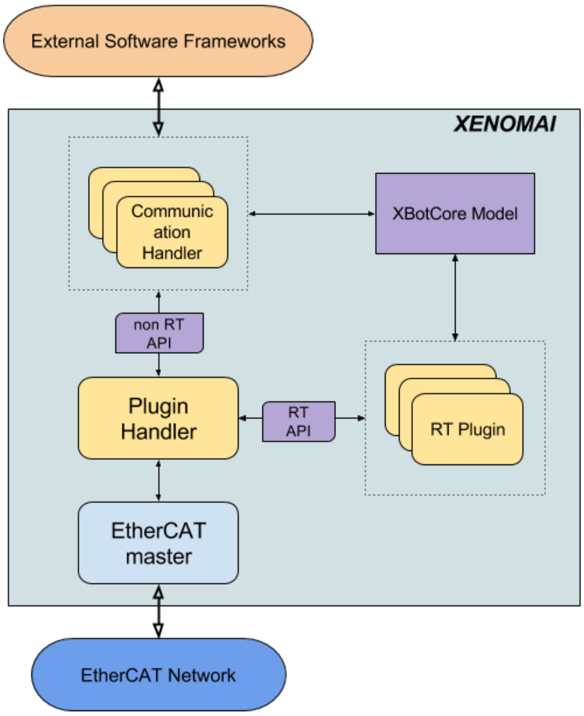

Figure 9: XBotCore components and relationships: EtherCAT slaves network, EtherCAT master implementation with one RT thread, Plugin handler for the RT plugin in the system with one RT thread, RT and non RT middleware API, Communication handlers for the external software frameworks integration.

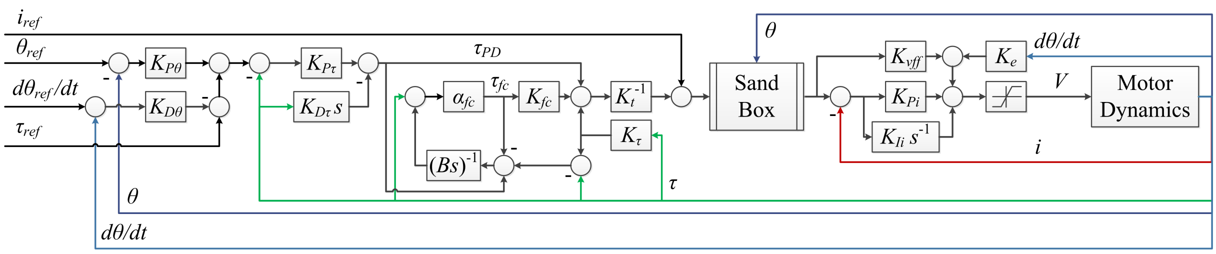

Figure 10: Block diagram scheme of the joint controllers: current feedback in red, torque feedback in green, position and velocity feedbacks in blue.

in Fig. 10. The inner most loop carry out the control of measured current i using a Proportional-Integral (PI) controller, with P and I gains of K_{Pi} and K_{Ii}. The current control execution is complemented by compensation of back-electromagnetic force (back-emf) effects with K_e denoting the back-EMF constant, and by addition of a voltage feed-forward term with a gain of K_{vff} on the current reference i_{ref}. The reference value i_{ref} is set by the torque controller when converted to current using the motor torque constant reflected to the rotor side, K_t, and by a centralised offset value i_{off}, provided that the joint position is within the admissible range. To respect the mechanical position limit of joints, we implement the "sand box" module. It includes a one-directional stiffening PD position controller that is activated when the joint position is approaching the end limit, and prevents the joint position from meeting the mechanical stop.

The torque controller is based on a Proportional-Derivative (PD) regulator, with P and D gains of $K_{P\tau}$ and $K_{D\tau}$, with a torque state feedback with a gain of K_τ. Furthermore, a friction compensation scheme [2, 7] is implemented for the cancellation of motor friction/damping, and a portion of estimated friction τ_{fc}, to be set by $K_{fc} \in [0, 1]$ is added to the torque controller output. This compensation scheme is on the basis of a first-order disturbance observer with a cut-off frequency of ω_{DOB} setting the compensation coefficient $\alpha_{fc} = \omega_{DOB} B$, with B denoting the reflected motor-side inertia of the actuator. The reference value for the torque controller is set from a decentralised torque offset τ_{off}, added to the output of the outer most controller, with P and D gains of $K_{P\theta}$ and $K_{D\theta}$, for position and velocity regulation around θ_{ref} and $\dot{\theta}_{ref}$.

6 Conclusions

This deliverable presented the first realization of the CENTAURO robot prototype. This first iteration of the robot was designed to satisfy the requirements of the system as originally described in the KHG meeting and detailed in deliverable D2.1 [4]. The robot body components were fabricated and the prototype has been successfully assembled and tested.

References

[1] Malgorzata Kamedula, Navvab Kashiri, Darwin G. Caldwell, and Nikos G. Tsagarakis. A Compliant Actuation Dynamics Gazebo-ROS Plugin for Effective Simulation of Soft Robotics Systems: Application to CENTAURO Robot. In *International Conference on Informatics in Control, Automation and Robotics*, volume 2, pages 485–491, Lisbon, Portugal, 2016.

[2] Kenji Kaneko, Shin'ichi Kondo, and Kouhei Ohnishi. A motion control of flexible joint based on velocity estimation. In *Annual Conference of IEEE Industrial Electronics Society*, pages 279–284, 1990.

[3] Navvab Kashiri, Arash Ajoudani, Darwin G. Caldwell, and Nikos G. Tsagarakis. Evaluation of Hip Kinematics Influence on the Performance of a Quadrupedal Robot Leg. In *International Conference on Informatics in Control, Automation and Robotics*, volume 1, pages 205–212. scitepress, 2016.

[4] Navvab. Kashiri, Houman. Dallali, and Nikos Tsagarakis. D2.1: Design concept of CENTAURO robot. 2015.

[5] Navvab Kashiri, Jorn Malzahn, and Nikos Tsagarakis. On the Sensor Design of Torque Controlled Actuators: A Comparison Study of Strain Gauge and Encoder Based Principles. *IEEE Robotics and Automation Letters*, 2(2):1186–1194, 2017.

[6] Navvab Kashiri, Nikos G Tsagarakis, Matteo Laffranchi, and Darwin G Caldwell. On the stiffness design of intrinsic compliant manipulators. In *IEEE/ASME International Conference on Advanced Intelligent Mechatronics*, pages 1306–1311, 2013.

[7] Luc Le Tien, Alin Albu-Schaffer, Alessandro De Luca, and Gerd Hirzinger. Friction observer and compensation for control of robots with joint torque measurement. pages 3789–3795. IEEE, 2008.

[8] Luca Muratore, Arturo Laurenzi, Enrico Mingo Hoffman, Alessio Rocchi, Darwin G. Caldwell, and Nikos G. Tsagarakis. XBotCore: A Real-Time Cross-Robot Software Platform. In *IEEE International Conference on Robotic Computing*, 2017.